Experimental Force Definition System for a New Orthodontic Retraction Spring

**Marcelo do Amaral Ferreira[a]; Fernando Torino de Oliveira[b];
Sérgio Aparecido Ignácio[c]; Paulo César Borges[d]**

Abstract: A new geometry of orthodontic retraction spring was experimentally studied through an electronic device (platform for measuring forces), using strain gauges that were adapted to cantilever beams. The sample consisted of 36 titanium-molybdenum springs, divided into three groups of 12 springs each. The springs were produced with different cross sections of 0.016×0.022 inch and 0.017×0.025 inch and with different angles between the extremities (120° and 130°). The springs were adapted to the platform in three different positions so that the force system developed by them could be known (horizontal forces, vertical forces, alpha-beta moments, and moment-to-force ratio M:F). The analysis of factorial variance and the Tukey honestly significant difference test were applied to verify the differences between the averages caused by three possible variation sources and the interactions between them. Regression analysis was also performed to obtain the spring rate. The results show the interactions between the three geometric variables, force magnitudes, and also the spring rates, which are compatible with the ones mentioned in the literature related to the subject. The spring rate was within the levels that are appropriate for clinical use (varying from $\beta = 33.1$ gf/mm to $\beta = 43.9$ gf/mm). (*Angle Orthod* 2005;75:368–377.)

Key Words: Retraction springs; Segmental arch; Anchorage unit

INTRODUCTION

Force systems resulting from complex geometric appliances produce forces and moments that determine the type of tooth movement. Force systems originating from orthodontic appliances have been studied by means of static systems[1–3] (simple springs, ie, cantilevers and palatal bars), complex systems (complex geometrical springs, ie, experimental[4–8] and numerical[9–13] approaches), or by means of dynamic systems (typodont system).[14] Numerical methods are the most recent approaches, having merged with the medical area due to computer science.[15] In experimental methods, the body of evidence is submitted to mechanical tests, which might determine the force system more accurately.

[a] Private Practice, Curitiba, Brazil.

[b] Undergraduate Student of Mechanical Engineering Course, CE-FET-PR, Curitiba, Brazil.

[c] Professor, Pontifical Catholic University of Paraná, Academic Department of Statistics, Curitiba, Paraná, Brazil.

[d] Professor, Federal Center of Technological Education of Paraná, Academic Department of Mechanics, Curitiba, Paraná, Brazil.

Corresponding author: Marcelo do Amaral Ferreira, DDS, MS, 1183 Prefeito Omar Sabbag Avenue, 80.210-000 Jardim Botânico, Curitiba, Paraná, Brazil
(e-mail: marcelo.ferreira@avalon.sul.com.br)

Three geometrical variables have been studied in this research: (1) cross section (CS), (2) theta angles (θA) formed between the alpha and beta extremities, and (3) delta position (ΔP). These variables have been chosen because they are the most influential in the performance of space closing loops in Orthodontics, as shown in previous studies.[8,13,16–22] The θA angles plus the loop position (in this case ΔP) are helpful in the production of differential moments. The delta that constitutes the body of the studied spring was based on the "Double Delta" loop[20] springs, which use a larger quantity of wire in their geometry.

Platforms[23–25] are electronic devices used for measuring forces in more than one direction and make it possible to determine the magnitude and direction of the resulting force exerted during a certain effort. In this study, a platform for measuring forces (Fy, Fx) and moments (Mz) produced by a new orthodontic retraction spring was developed.

Force level

Burstone[26] advised that "T-loops" (0.017×0.025 inch, TMA) attraction springs must be kept below 300 g to minimize anterior retraction and produce posterior protraction. Braun et al[6] studied forces developed by centered T-loops (0.017×0.025 inch, TMA) and reported forces that varied from 50 to 300 g. Braun and Marcotte[16] also studied centered T-loop (0.017×0.025 inch, TMA) and reported forces that varied from 50 to 350 g.

TABLE 1. Spring Groups, Theta Angles, Cross Sections, and Samples

Delta Position (ΔP)	Theta Angle (θA)	Cross Section (CS)	Sample	Running Tests
Alpha	120°	0.016 × 0.022-inch	3	10
		0.017 × 0.025-inch	3	10
	130°	0.016 × 0.022-inch	3	10
		0.017 × 0.025-inch	3	10
Beta	120°	0.016 × 0.022-inch	3	10
		0.017 × 0.025-inch	3	10
	130°	0.016 × 0.022-inch	3	10
		0.017 × 0.025-inch	3	10
Centered	120°	0.016 × 0.022-inch	3	10
		0.017 × 0.025-inch	3	10
	130°	0.016 × 0.022-inch	3	10
		0.017 × 0.025-inch	3	10

TABLE 3. Accepted Deviations and Spring Dimensions

Especification	Tolerances	Dimension 1	Dimension 2
Helix (diameter, mm)	± 0.1	3	3
Height (mm)	± 0.1	8	8
Angle Δ (°)	± 1	60	60
Angle θ (°)	± 1	130	120
Length (mm)	± 0.5	24	24

Moment-to-force ratios (M:F)

According to Braun et al,[6] an M:F ratio of approximately 10 mm must be applied to the anterior and posterior teeth to achieve a translatory force system. To achieve posterior protraction, a larger moment should be applied to the anterior teeth (M:F approximating 12–13 mm), and reversing the force system would produce anterior retraction. Siatkowski[11] reported an M:F ratio of 8.4 mm, capable of producing translation of the maxillary anterior teeth and an M:F varying from 8.2 mm to 8.5 mm for the maxillary posterior teeth.

Spring rate

Fryar[8] studied a single "vertical helical torsion" spring (0.008 × 0.020 inch, SS) and reported that the load-deflection rate averaged 12 g/mm (10 mm height). Burstone et al[17] investigated centered T-loops (0.017 × 0.025 inch, TMA) and found a mean spring rate of 55 g/mm. Yang and Baldwin[19] analyzed the behavior of "Bull" and "Vertical" loops (0.017 × 0.022 inch, SS) and found a mean spring rate of 57 and 114 g/mm, respectively. Gjessing[27] developed a spring (0.016 × 0.022 inch, SS) with a spring rate
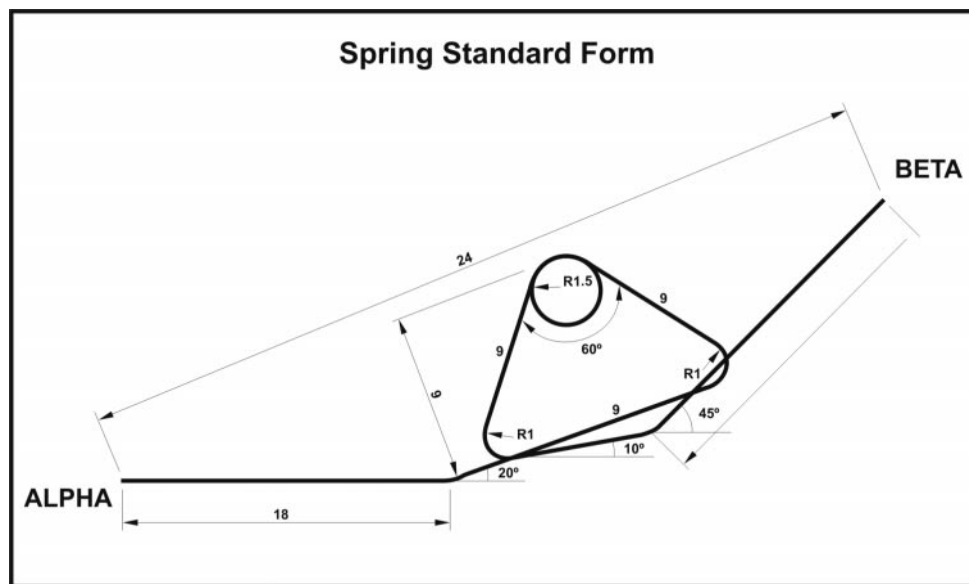

FIGURE 1. Retraction spring standard form (mm).

TABLE 2. Wire Material, Cross Section, Yield Strength ($\sigma\theta$), and Elastic Modulus (E)[a]

Wire Material	Cross Section (mm²)	Yield Strength ($\sigma\theta$) (Mpa)	Elastic Modulus (E) 10^4 (Gpa)
Titanium-molybdenum (β-titanium)	0.406 × 0.559 mm (0.016 × 0.022-inch)	1380 (200 × 10^3 psi)	69 (10 × 10^6 psi)
Titanium-molybdenum (β-titanium)	0.432 × 0.635 mm (0.017 × 0.025-inch)	1240 (180 × 10^3 psi)	69 (10 × 10^6 psi)

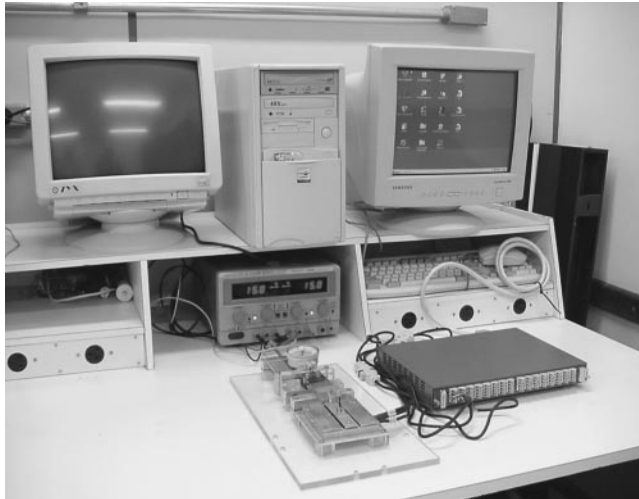[a] Source: Ormco Corp, Glendora, Calif.

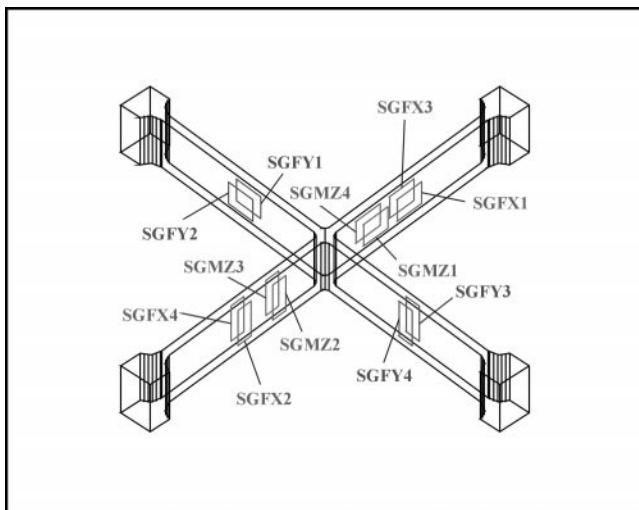**FIGURE 2.** Platform and data acquisition set.

FIGURE 3. Internal part of the platform, depicting the cross-shaped beam and Strain gauge display.

of 45 g/mm. Bench et al[28] verifying "Double Vertical Helical" closing loops (0.016 × 0.016 inch, Co-Cr) found a spring rate of 75 g/mm.

MATERIALS AND METHODS

Sample

The sample consisted of 36 springs made in titanium-molybdenum wire (TMA, Ormco Corp, Glendora, Calif) divided into three spring groups (Alpha Spring Group—ASG, Beta Spring Group—BSG, and Centered Spring Group—CSG). Each group presented 12 springs, with different end angles (120° and 130°) and different CSs, 0.016 × 0.022 inch and 0.017 × 0.025 inch. Each spring was submitted to 10 measurements, involving 30 repetitions (Table 1). The spring geometry consists of a delta form with one-and a half-turn helix in its superior portion and gable
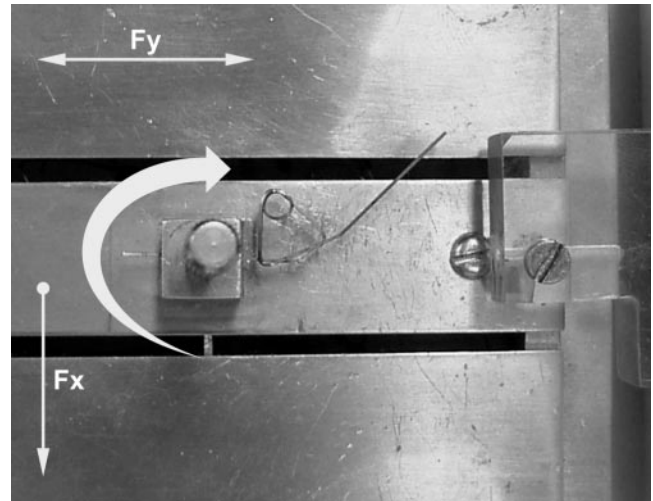
FIGURE 4. Adapted retraction spring with the delta close to the responsive fitting (Alpha Spring Group).
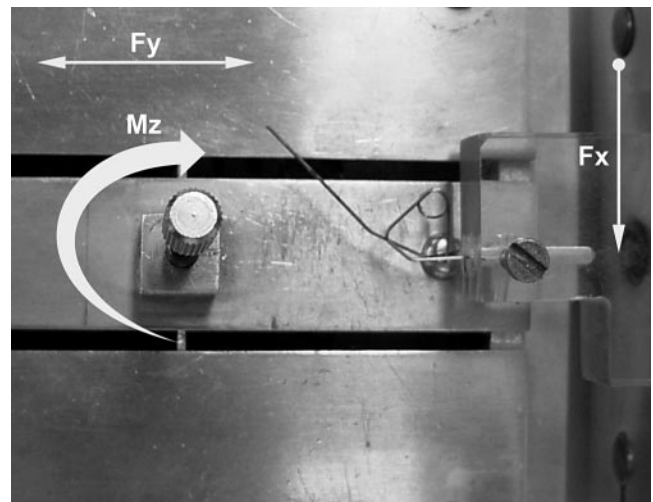

FIGURE 5. Adapted retraction spring with the delta close to the nonresponsive fitting (Beta Spring Group).

bends (120° or 130°). Figure 1 illustrates schematically the described geometry.

Table 2 shows wire material properties. The spring features were inspected in relation to their reproducibility in a profile projection device (Projection Screen 560 × 460 mm, accuracy of magnification 0.5%; working scale ±0.1 mm, Henri Hauser SA, Bienne, Suisse). Only the springs whose angular and linear dimensions were within the established tolerance limit were tested (Table 3). The following geometrical parameters were defined.

- CS.
- Theta Angle (θA) formed between the alpha and beta extremities.
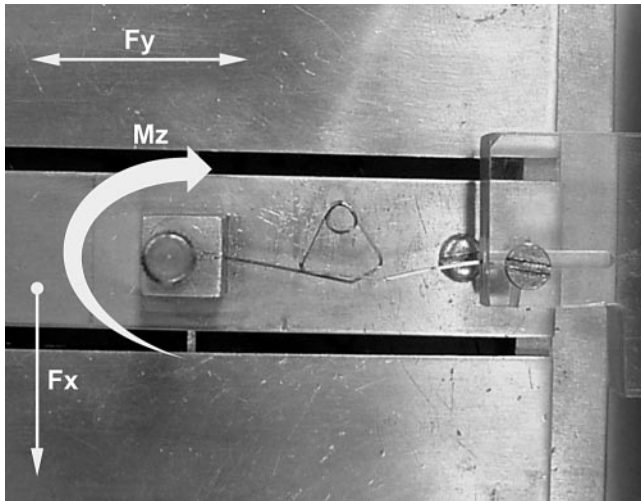- Delta position (ΔP).

FIGURE 6. Adapted retraction spring positioned equally spaced (Centered Spring Group).

Apparatus

A platform for measuring forces and moments has been developed jointly by the Integrated Laboratory of Materials, Federal Center of Technological Education of Paraná (CE-FET-PR) and the Laboratory of Applied Mechanics, Federal University of Rio Grande do Sul (UFRGS). The plat-

form is capable of measuring forces and moments produced by a closing loop. In this study, it was established that Fy forces are caused by the activation of the spring in the horizontal direction, whereas Fx forces indicate the vertical forces, which are perpendicular to Fy. Finally, the Mz moment represents a rotational tendency due to the inclinations that occur in the extremities of the spring. The platform (Figure 2 shows the platform and data acquisition set), a home-made aluminum structure (AI2024T3), is made up of a cross-shaped beam tied to its internal part, with 12 strain gauges (SG). Figure 3 shows the SG, in the cross-shaped beam, for the measurement of Fx, Fy, and Mz. The platform provides a scale rate of 1 kgf, a supply source of 5 V, and data acquisition system (A/D) of ± 5 V. SG of Mz and Fx are double (model EA-13-060PB-120, Texas Measurements Inc, Dallas, TX), and the SG of Fy are simple uniaxial (model KFG-2N-120-CI-23, Soltec Corporation, San Fernando, CA).The system was calibrated with dead weights up to 500 g.

Procedure

The springs were adapted for testing (the spring being mounted in one extremity and freely dislocated in the other) in the platform in the following way.

The delta was dislocated three mm toward the responsive

TABLE 4. Descriptive Statistics, Means of Fy, Fx, and Mz by CS, θA, and ΔP

| | Treatment Average | | | | | | |
| | Cross Section | | Angle θ (°) | | Delta Position | | |
Source	0.406 × 0.559 (mm) (0.016 × 0.022-inch)	0.432 × 0.635 (mm) (0.017 × 0.025-inch)	120	130	Alpha	Beta	Centered
$Fy_{(0.0)gf}$	−21.9	−27.3	−33.4	−15.8	−25.7	−20.7	−27.5
$Fy_{(3.0)gf}$	−19.9	−24.8	−29.6	−15.1	−22.3	−15.1	−29.7
$Fy_{(6.0)gf}$	−22.8	−25.3	−30.7	−17.4	−28.5	−11.7	−31.9
$Fx_{(0.0)gf}$	−4.0	−10.9	−7.5	−7.5	−11.7	−16.8	6.0
$Fx_{(3.0)gf}$	103.5	113.3	109.2	107.6	101.7	108.3	115.2
$Fx_{(6.0)gf}$	208.9	252.9	230.8	230.9	234.7	231.5	226.5
$Mz_{(0.0)gf/mm}$	842.9	899.8	1052.2	690.4	747.6	734.3	1132.1
$Mz_{(3.0)gf/mm}$	954.0	1127.7	1147.8	934.0	1124.2	654.0	1344.5
$Mz_{(6.0)gf/mm}$	1011.8	1223.2	1194.6	1040.4	1348.8	563.1	1440.5

TABLE 5. Three-Way ANOVA Summary Table for the Data Variables Fy[a]

| | Fy (0.0) | | Fy (3.0) | | Fy (6.0) | |
Variables	F	P value	F	P value	F	P value
CS (A)	18.2241	.0000**	10.5990	.0012**	350.5276	.0000**
θA (B)	0.0013	.9713 NS	0.2888	.5913 NS	0.0009	.9762 NS
ΔP (C)	72.8614	.0000**	6.6522	.0150*	4.0858	.0170*
A × B	52.2869	.0000**	17.6313	.0000**	5.9957	.0148*
A × C	3.1822	.0427*	5.1850	.0060**	17.5286	.0000**
B × C	54.4643	.0000**	2.9886	.0517 NS	14.3878	.0000**
A × B × C	26.5131	.0000**	19.2461	.0000**	15.6430	.0000**

* $P \leq .05$.

** $P \leq .01$.

[a] CS indicates cross section; ANOVA, analysis of variance; NS, not significant; θA, Theta angles; and ΔP, Delta positions.

TABLE 6. Three-Way ANOVA Summary for the Data Variable Fx[a]

	Fx (0.0)		Fx (3.0)		Fx (6.0)	
Variables	F	P Value	F	P Value	F	P Value
CS (A)	20.7844	.0000**	29.510	.0000**	9.105	.0027**
θA (B)	224.0730	.0000**	248.224	.0000**	247.0719	.0000**
ΔP (C)	11.8641	.0000**	85.1057	.0000**	215.4760	.0000**
A × B	2.6105	.1071 NS	1.3880	.2395 NS	0.0002	.9888 NS
A × C	25.1822	.0000**	1.4975	.2251 NS	3.6844	.0261*
B × C	31.2237	.0000**	44.3957	.0000**	31.0728	.0000**
A × B × C	5.5097	.0044**	2.6845	.0697 NS	2.1627	.1166 NS

* $P \leq .05$.
** $P \leq .01$.
[a] CS indicates cross section; ANOVA, analysis of variance; NS, not significant; θA, Theta angles; and ΔP, Delta positions.

TABLE 7. Three-Way ANOVA Summary for the Data Variable Mz[a]

	Mz (0.0)		Mz (3.0)		Mz (6.0)	
Variables	F	P value	F	P value	F	P value
CS (A)	9.5129	.0022**	60.6625	.0000**	69.5165	.0000**
θA (B)	383.9093	.0000**	91.8705	.0000**	37.0010	.0000**
ΔP (C)	199.6572	.0000**	333.4933	.0000**	482.2162	.0000**
A × B	33.3685	.0000**	13.4742	.0003**	10.0515	.0017**
A × C	92.8804	.0000**	81.2386	.0000**	86.7060	.0000**
B × C	32.7698	.0000**	11.2376	.0000**	8.8756	.0002**
A × B × C	47.5711	.0000**	54.3041	.0000**	28.9054	.0000**

* $P \leq .05$.
** $P \leq .01$.
[a] CS indicates cross section; ANOVA, analysis of variance; NS, not significant; θA, Theta angles; and ΔP, Delta positions.
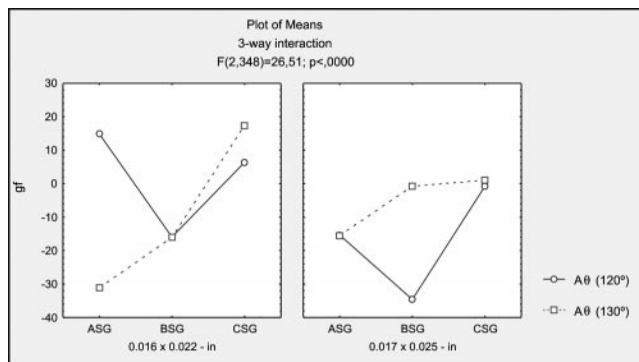

FIGURE 7. Fy(0.0) Cross section, delta position, and theta angle interaction.
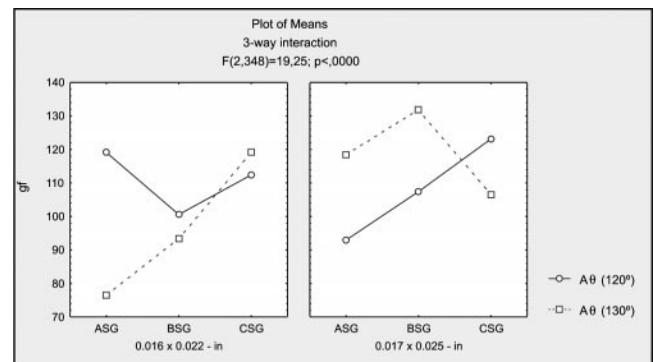

FIGURE 8. Fy(3.0) Cross section, delta position, and theta angle interaction.

fitting of the device to study the force system acting on the alpha extremity in an asymmetrical approach (ASG) (Figure 4).

The spring was reversed and the delta was dislocated three mm toward the nonresponsive fitting of the device to study the force system acting on the beta extremity in an asymmetrical approach (BSG) (Figure 5).

The delta was reset equidistant from the fixing points (CSG) (Figure 6).

Statistical analysis

To identify differences between the averages produced by three possible variation sources (independent variables) and the interactions between them (CS, ΔP, and θA), a three-factor analysis of variance (ANOVA) was performed (complete factorial) (Table 4). Tables 5–7 show the results of ANOVA. The Tukey honestly significant difference test was also used to determine multiple comparisons between the main effects and their interactions.
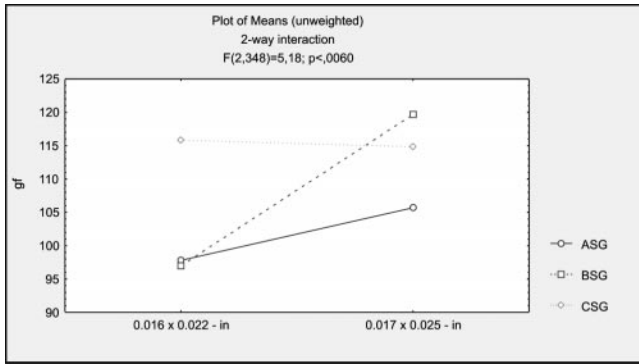
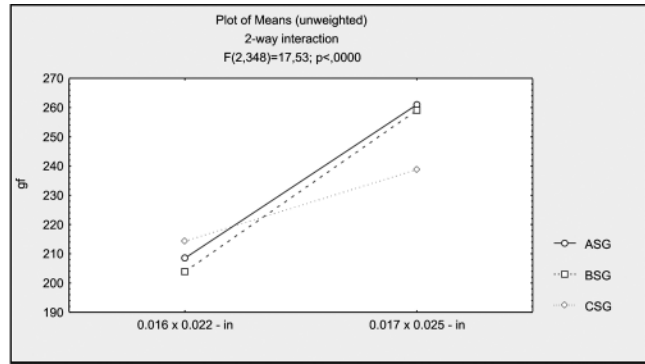**FIGURE 9.** Fy(3.0) Cross section and delta position interaction.

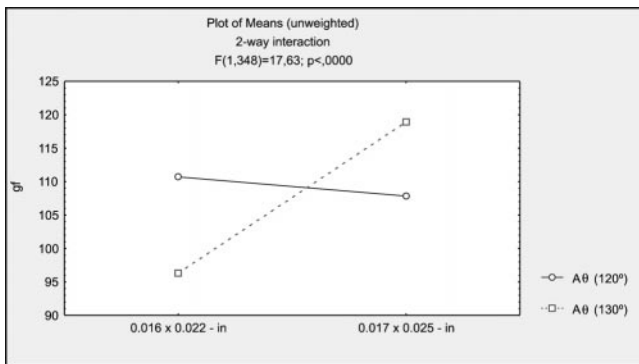**FIGURE 12.** Fy(6.0) Cross section and delta position interaction.

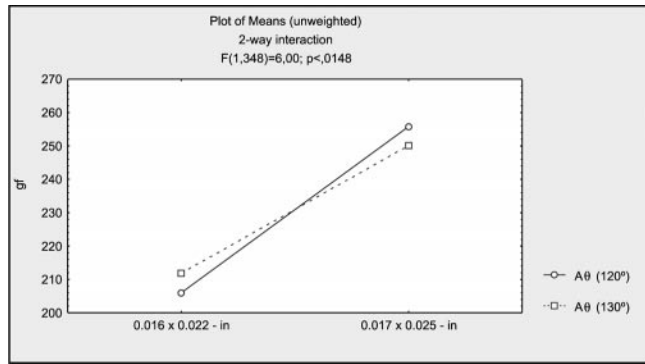**FIGURE 10.** Fy(3.0) Cross section and theta angle interaction.

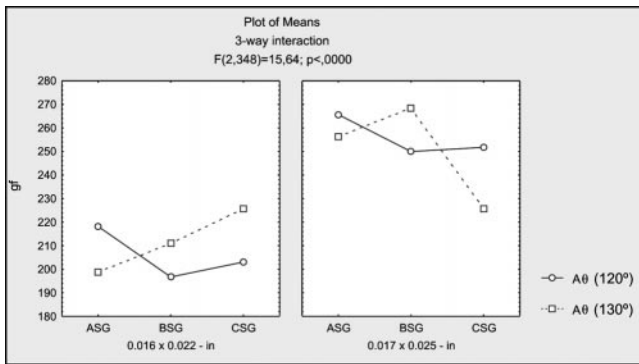**FIGURE 13.** Fy(6.0) Cross section and theta angle interaction.

FIGURE 11. Fy(6.0) Cross section, delta position, and theta angle interaction.

RESULTS

General comparison of the samples

For Fy at rest and Fy at six mm activation, only the θA (120° or 130°) variable has not shown any influence on the results obtained. For Fy at three mm activation, it was observed that there was no statistically significant difference for the θA variable, and there was no interaction between the variables $\Delta P - \theta A$. For Fx at rest, there was no inter-

action between CS and θA. For Fx at three mm, there was no interaction between $CS - \Delta P$, $CS - \theta A$, and between $CS - \Delta P - \theta A$. For Fx six mm, there was no interaction between $CS - \theta A$ and between $CS - \Delta P - \theta A$. Toward moment Mz, all variables proved to be significant to explain the variations at Mz. ($P \leq .05$) (Tables 5–7).

Comparison of the samples through Tukey test

There was a statistically significant difference between the variables studied for Fy, Fx, and Mz at rest and at three and six mm activation through Tukey analysis (Table 4).

It has been noticed that

- the CS variable was relevant for Fx, Fy, and Mz forces for the activation values studied;
- the angle variable (θA) was relevant for Fx and Mz for the activation values studied;
- the delta position (ΔP) variable was relevant for Fx (rest) forces between ASG and BSG and between BSG and CSG; for Fy rest and Fx (three and six mm), it was relevant among the spring groups; for Fy (three and six mm) was relevant for ASG and CSG; and for Mz (three and six mm), it has been relevant for all the spring groups. The value of Mz (rest) was relevant between ASG and CSG and between BSG and CSG. The behavior of geo-

TABLE 8. Average Force Level

Activation (mm)	Fy (gf)					
	0.016 × 0.022-inch α, 120°	0.016 × 0.022-inch α, 130°	0.017 × 0.025-inch α, 120°	0.017 × 0.025-inch α, 130°	0.016 × 0.022-inch β, 120°	0.016 × 0.022-inch β, 130°
0	14.8	−31	−15.3	−15.5	−15.9	−15.9
1	51	5	36	29	41	25
2	85	42	82	75	72	62
3	119	76.4	92.9	118.4	110.5	93.3
4	153	116	175	166	133	136
5	187	154	221	211	164	173
6	218	199	266	256	197	211

TABLE 9. Spring Groups M:F Ratios Vs Activation

Spring Activation (mm)	M:F (mm)					
	Mα/Fy 0.016 × 0.022-inch (120°)	Mα/Fy 0.016 × 0.022-inch (130°)	Mβ/Fy 0.016 × 0.022-inch (120°)	Mβ/Fy 0.016 × 0.022-inch (130°)	MC/Fy 0.016 × 0.022-inch (120°)	MC/Fy 0.016 × 0.022-inch (130°)
0	∞	∞	∞	∞	∞	∞
1	∞	∞	∞	∞	∞	∞
2	13.9	14.4	15.0	10.0	16.7	12.4
3	10.1	8.2	9.6	6.0	9.9	10.3
4	8.1	7.7	8.3	5.1	9.1	7.5
5	6.8	5.2	6.7	3.6	7.2	6.1
6	6.0	4.6	4.7	2.1	5.5	5.7

metrical variables interaction of the spring groups studied is shown graphically in Figures 7–13.

Force level

The force levels found in all the spring groups studied have varied from an average of 34 gf to 230 gf (one to six mm activation, respectively). The negative values found for Fy (rest) reveal compressive forces over the springs,[1] due to friction, because they are adapted into the transducer. However, they are of low magnitude and can be disregarded (Table 8).

The M:F ratio

Concerning ASG (0.016 × 0.022 inch, 130°), the Mα:Fy at four mm activation is equal to 7.7 mm, and Mα:Fy is 8.2 mm at three mm activation. Finally, Mα:Fy reaches 14.4 mm at two mm activation. At five mm activation, the Mα:Fy ratio is 5.2 mm. For ASG (0.017 × 0.025 inch, 120°), the Mα:Fy has varied from 6.1 to 6.7 mm at six and five mm activation, respectively. The Mα:Fy increases from 8.4 to 15.0 mm when the spring is deactivated at three mm and becomes stable at two mm activation (Mα:Fy is 15.4 mm). For BSG (0.017 × 0.025 inch, 120° and 0.017 × 0.025 inch, 130°), the Mβ:Fy ratios have been shown to be low, from three mm activation up to six mm. The CSG (0.017 × 0.025 inch) with 120° end angles has shown that the Mc:Fy ratio is altered from 6.9 mm at six mm activation to 9.6 mm at five mm activation and to 11.5 mm at four mm activation. Springs with 130° end angles have shown less sudden alterations during deactivation (Table 9).

TABLE 10. Estimated Coefficient of Spring Rate and Standard Error

Variables	Estimate of Angular Coefficient β_1	Standard Error	t_0	P value	F_0	P value	R^2	S_{yx}
Alpha 0.017 × 0.025-inch (120°)	43.9	1.9	22.8	.0000	521.6	.0000	0.9	31.7
Alpha 0.017 × 0.025-inch (130°)	41.7	1.5	26.9	.0000	725.2	.0000	0.9	25.6
Beta 0.016 × 0.022-inch (120°)	33.1	1.2	26.7	.0000	715.8	.0000	0.9	20.4
Beta 0.017 × 0.025-inch (130°)	38.0	3.5	10.6	.0000	112.7	.0000	0.8	59.2
Centered 0.016 × 0.022-inch (120°)	34.4	1.1	29.7	.0000	882.5	.0000	0.9	19.1
Centered 0.016 × 0.022-inch (130°)	38.3	0.8	47.1	.0000	2226.0	.0000	0.9	13.4
Centered 0.017 × 0.025-inch (120°)	36.8	2.9	12.3	.0000	153.0	.0000	0.8	49.1
Centered 0.017 × 0.025-inch (130°)	37.2	0.8	42.2	.0000	1785.3	.0000	0.9	14.5

$P \leq .05.$

TABLE 8. Extended

Fy (gf)					
0.017 × 0.025-inch β, 120°	0.017 × 0.025-inch β, 130°	0.016 × 0.022-inch C, 120°	0.016 × 0.022-inch C, 130°	0.017 × 0.025-inch C, 120°	0.017 × 0.025-inch C, 130°
−34.5	−0.8	6.3	17.3	−0.7	1.0
14	43	41	45	44	37
61	80	73	81	79	74
107	131.9	117.3	114	123	106
156	153	139	154	148	149
203	189	171	191	183	186
250	268	203	226	252	226

TABLE 9. Extended

M:F (mm)					
Mα/Fy 0.017 × 0.025-inch (120°)	Mα/Fy 0.017 × 0.025-inch (130°)	Mβ/Fy 0.017 × 0.025-inch (120°)	Mβ/Fy 0.017 × 0.025-inch (130°)	MC/Fy 0.017 × 0.025-inch (120°)	MC/Fy 0.017 × 0.025-inch (130°)
∞	∞	∞	∞	∞	∞
∞	∞	∞	∞	∞	∞
15.4	16.0	10.3	9.3	19.0	16.2
15.0	10.6	4.5	4.5	13.8	12.4
8.4	8.8	3.0	4.3	11.5	9.6
6.7	7.3	2.0	3.1	9.6	8.1
6.1	6.3	1.5	1.7	6.9	6.9

TABLE 11. Mα:F Ratio Results Vs Literature Review

Activation (mm)	Burstone[26] 0.018–0.017 × 0.025-inch Mα:F "Composite Canine Retraction Spring"	Gjessing[27] Stainless Steel 0.016 × 0.022-inch "Ovoide Double Helix Loop"	Burstone et al[17] TMA 0.018-0.017 × 0.025-inch "Composite Canine Retraction"	Braun et al[6] TMA 0.017 × 0.025-inch "T-Loop"	Mα:Fy TMA 0.016 × 0.022 (120°)	Mα:Fy TMA 0.017 × 0.025 (120°)	Mα:Fy TMA 0.017 × 0.025 (130°)
0	0.0	12.5	∞	—	∞	∞	∞
1	12.6	10.0	∞	—	∞	∞	∞
2	8.4	—	7.0	—	13.9	15.4	16.0
3	7.1	—	5.8	—	10.1	15.0	10.6
4	6.4	—	5.3	10.0	8.1	8.4	8.8
5	6.0	—	5.2	—	6.8	6.7	7.3
6	5.6	—	4.9	—	6.0	6.1	6.3

TABLE 12. Mβ:F Ratio Results Vs Literature Review

Activation (mm)	Burstone[26] 0.018–0.017 × 0.025-inch Mβ:F "Composite Canine Retraction Spring"	Burstone et al[17] 0.018-0.017 × 0.025-inch Mβ:F "Composite Anterior Retraction Spring" (Long)	Mβ:Fy 0.016 × 0.022 (120°)	Mβ:Fy 0.016 × 0.022 (130°)	Mβ:Fy 0.017 × 0.025 (120°)	Mβ:Fy 0.017 × 0.025 (130°)
0	0	—	∞	∞	∞	∞
1	74.7	23.7	∞	∞	∞	∞
2	35.9	13.8	15.0	10.0	10.3	9.3
3	24.3	10.2	9.6	6.0	4.5	4.5
4	18.6	8.4	8.3	5.1	3.0	4.3
5	15.2	7.6	6.7	3.6	2.0	3.1
6	12.8	6.8	4.7	2.1	1.5	1.7

TABLE 13. Mc:F Ratio Results Vs Literature Review

Activation (mm)	Burstone[26] TMA 0.017 × 0.025-inch "Centered T-Loop"	Braun and Marcotte[16] TMA 0.017 × 0.025-inch "T-Loop"	Burstone et al[17] TMA 0.017 × 0.025-inch "Centered T-Loop"	Raboud et al[13] TMA 0.017 × 0.025-inch "T-Loop"
0	∞	—	∞	—
1	31.2	31.0	∞	—
2	18.2	18.0	12.9	13.7[a]
3	13.3	—	9.7	—
4	10.9	11.0	8.0	8.4[b]
5	9.2	—	6.9	—
6	8.0	8.0	6.0	—

[a] At ½ max.activation.
[b] Max.activation at 4.5 mm.

Spring rate

This study has shown a spring rate variation from 33.1 to 43.9 gf/mm depending on the spring group studied (Table 10).

DISCUSSION

Geometry

An apical helix has been included inside the delta to reduce a concentration of efforts and to produce a greater spring effect. When the spring is activated, the delta sides come closer, becoming almost parallel at the maximum activation studied (six mm). In this way, a greater range of activation can be found because the spring is activated in the same direction as the original bending.[18]

Force level

The average values found have shown a force magnitude varying from 34 gf to 230 gf, which is slightly lower than the forces described by Braun et al.[6] The ASG 0.016 × 0.022 inch, 120°, has stored 119 gf at three mm activation, whereas ASG 0.017 × 0.025 inch, 130°, has stored 118 gf. These forces agree with Burstone et al[17] (composite spring 0.017 × 0.025 inch, TMA, long). For T-loops with asymmetrical angulations to produce posterior protraction, they found 230 g (three mm activation) and 466 g (six mm activation). The BSG 0.016 × 0.022 inch, 120°, has stored 110.5 gf (three mm activation) and 197 gf (six mm activation). Braun and Marcotte[17] (T-loops, 0.017 × 0.025 inch, TMA) found forces that varied from 50 g (one mm activation) to 350 g (eight mm activation), whereas this study shows average force levels that are slightly lower (for CSG 0.017 × 0.025 inch, 130°). Similar values were found for CSG 0.017 × 0.025 inch, 120°.

The M:F ratio

The data obtained were the result of an experiment, so they may not reflect clinical conditions exactly. However, the spring groups studied might be analyzed in relation to the M:F developed by them. The ASG (0.017 × 0.025 inch, 130°) produced an Mα:F compatible with translation at

three mm activation and an Mα:F compatible with uncontrolled tipping at six mm activation. At two and four mm activation, these springs showed an Mα:F equal to 16.0 and 8.8 mm, respectively. The values of ASG (0.017 × 0.025 inch, 120° and 130°) are slightly above the ones found by Burstone[26] (Table 11). The BSG (0.016 × 0.022 inch, 130°; 0.017 × 0.025 inch, 120°; and 0.017 × 0.025 inch, 130°) has shown very low Mβ:Fy ratios, which makes these groups undesirable for protraction movements.[17] This is something that has not taken place in relation to 0.016 × 0.022 inch, 120° springs, which have proven to be appropriate at five mm activation and reactivated before two mm (Table 12). In this study, the Mc:F ratio is compatible with translation (from five to four mm activation) and with root movement (at three mm activation) for 0.017 × 0.025 inch, 120° and 130° springs (Table 13).

Spring rate

The ASG (0.017 × 0.025 inch) has shown the highest spring rates (42.8 gf/m, average), which is slightly above the value found by Burstone[26] (33 g/mm), for the composite T-loop and which is slightly lower in relation to the centered T-loops (0.017 × 0.025 inch, TMA) studied by Burstone et al[17] (approximately 55 g/mm). The canine-retraction developed by Gjessing[27] stored 45 g/mm. Yang and Baldwin[19] found 57 g/mm ("Bull loop"), whereas BSG (0.017 × 0.025 inch) has shown 38 gf/mm. The CSG (0.017 × 0.025 inch) has shown a mean 37 gf/mm. The values found in the spring groups studied are within compatible levels. While comparing such outcomes, it is important to emphasize that the cross section, wire material, and loop geometry have strong influence on the spring rate definition.

CONCLUSIONS

- The highest force levels were found in the 0.017 × 0.025-inch spring groups.
- BSG (0.016 × 0.022 inch, 130°) springs have shown the lowest force levels.
- BSG (0.016 × 0.022 inch, 130°) and BSG (0.017 ×

TABLE 13. Extended

Braun et al[6] TMA 0.017 × 0.025-inch "Centered T-Loop"	MC:Fy 0.017 × 0.025-inch (120°)	MC:Fy 0.017 × 0.025-inch (130°)	MC:Fy 0.016 × 0.022-inch (120°)	MC:Fy 0.016 × 0.022-inch (130°)
31	∞	∞	∞	∞
17.5	∞	∞	∞	∞
—	19.0	16.2	16.7	12.4
13.0	13.8	12.4	9.9	10.3
—	11.5	9.6	9.1	7.5
—	9.6	8.1	7.2	6.1
9.0	6.9	6.9	5.5	5.7

0.025 inch, 120° and 130°) springs have shown very low M:F relations.

- M:F relations tend to decrease as activation values increase.
- The delta centricity affects the M:F ratios in alpha, beta, and centered positions.
- In this study, spring rates varying from 33.1 gf/mm to 43.9 gf/mm have been found.

ACKNOWLEDGMENT

REFERENCES

1. Braun S, Garcia JL. The gable bend revisited. *Am J Orthod Dentofacial Orthop.* 2002;122:523–527.
2. Peyton FA, Moore GR. Flexibility studies on gold alloy wires and orthodontic appliance. *Int J Orthod.* 1933;19:903–919.
3. Choy K, Pae E, Park YC, Burstone CJ. Controlled space closure with a statically determinate retraction system. *Angle Orthod.* 2002;72:191–198.
4. Nägerl H, Burstone CJ, Becher B, Messenburg DK. Center of rotation with transverse forces: an experimental study. *Am J Orthod Dentofacial Orthop.* 1991;99:337–345.
5. Ferreira MA. The wire material and cross-section effect on double delta closing loops regarding load and spring rate magnitude: an *in vitro* study. *Am J Orthod Dentofacial Orthop.* 1999;115:275–282.
6. Braun S, Sjursen RC, Legan HL. On the management of extraction sites. *Am J Orthod Dentofacial Facial Orthop.* 1997;112:645–655.
7. Solonche DJ, Burstone CJ, Vanderby R. A device for determining the mechanical behavior of orthodontic appliances. *IEEE Trans Biomed Eng.* 1977;24:538–539.
8. Fryar GM. *Load-Deflections Determinations of Specific Wire Configurations* [master's thesis]. Indianapolis, Ind: University of Indiana; 1960.
9. Ferreira MA, Orlowski R, Luersen MA, Borges PCB. Análise do desempenho de alças de retração ortodôntica via método dos elementos finitos. *Anais.* XVII CBEB 2000. Florianópolis, Brasil. Setembro.
10. Rinaldi TC, Johnson BE. An analytical evaluation of a new spring design for segmented space closure. *Angle Orthod.* 1995;65:187–198.
11. Siatkowski RE. Continuous arch wire closing loop design, optimization, and verification. Part I. *Am J Orthod Dentofacial Orthop.* 1997;112:393–402.
12. Siatkowski RE. Continuous arch wire closing loop design, optimization, and verification. Part II. *Am J Orthod Dentofacial Orthop.* 1997;112:487–495.
13. Raboud DW, Faulkner MG, Lipsett AW, Haberstock DL. Three-dimensional effects in retraction appliance design. *Am J Orthod Dentofacial Orthop.* 1997;112:378–392.
14. Rhee J, Chu Y, Row J. A comparison between friction and frictionless mechanics with a new typodont simulation system. *Am J Orthod Dentofacial Orthop.* 1997;119:292–299.
15. Luersen MA. *Introdução ao método dos elementos finitos.* Curitiba, Brazil: Centro Federal de Educação Tecnológica do Paraná, Março, 1999.
16. Braun S, Marcotte MR. Rationale of the segmented approach to orthodontic treatment. *Am J Orthod Dentofacial Orthop.* 1995;108:1–8.
17. Burstone CJ, Steenbergen E, Hanley K. *Modern Edgewise Mechanics and the Segmented Arch Technique.* Farmington, Conn: University of Connecticut Health Center; 1995.
18. Burstone CJ, Baldwin JJ, Lawless DT. The application of continuous forces to orthodontics. *Angle Orthod.* 1961;31:1–14.
19. Yang TY, Baldwin JJ. Analysis of space closing springs in orthodontics. *J Biomech.* 1974;7:21–28.
20. Ricketts RM. Bioprogressive therapy as an answer to orthodontic needs. Part II. *Am J Orthod* 1976;70:241–268.
21. Kuhlberg AJ, Burstone CJ. T-loop position and anchorage control. *Am J Orthod Dentofacial Orthop.* 1997;112:12–18.
22. Bourauel C, Drescher D, Ebling J, Broome D, Kanarachos A. Superelastic nickel titanium alloy springs—an investigation of force systems. *Eur J Orthod.* 1997;19:491–500.
23. Desjardins P, Gagnon M. A force platform for large human displacement. *Med Eng Phys.* 2001;23:143–146.
24. Yarrow K, Brown P, Gresty MA, Bronstein AM. Force platform recordings in the diagnosis of primary orthostatic tremor. *Gait Posture.* 2001;13:27–34.
25. Fairburn PS, Palmer R, Whybrow J, Fielden S, Jones S. A prototype system for testing force platform dynamic performance. *Gait Posture.* 2000;12:25–33.
26. Burstone CJ. The segmented approach to space closure. *Am J Orthod.* 1982;82:361–378.
27. Gjessing P. Biomechanical design and clinical evaluation of a new canine retraction spring. *Am J Orthod.* 1985;87:353–362.
28. Bench RW, Gugino CF, Hilgers JJ. Bioprogressive therapy. *JCO.* 1978;12:123–139.